

7. PLEISTOCENE AGE MODELS, LEG 150¹

Beth A. Christensen,² B.W. Hoppie,³ R.C. Thunell,² K.G. Miller,^{4,5} and L. Burckle⁵

ABSTRACT

Leg 150 drilling on the New Jersey slope recovered thick (110–350 m) middle Pleistocene sections at Sites 902 (811 m water depth), 903 (444 m), and 904 (1123 m). The physical properties records (gamma-ray attenuated porosity evaluator [GRAPE] and magnetic susceptibility) show distinct glacial–interglacial changes. Ages for these sections are constrained by calcareous nannofossil datums. A stratigraphy for each site was established by using GRAPE and magnetic susceptibility data that were calibrated to the SPECMAP oxygen isotope time scale (Imbrie et al., 1984). We improved the shipboard chronologies by tuning the physical properties records to the SPECMAP $\delta^{18}\text{O}$ stack in order to generate astronomically tuned stratigraphies for Sites 902, 903, and 904 at the oxygen isotope substage level. There is a high degree of similarity between the records at Sites 902, 903, and 904, despite the fine-scale variability unique to each hole. The most complete physical properties records are at Site 902, which provides the foundation for the Leg 150 studies. We extend the relationships established at Site 902 to Sites 903 and 904.

Spectral and cross-spectral analysis of the tuned records were performed on the physical properties and the SPECMAP records. These analyses provide statistical evidence for the correlation of GRAPE and the SPECMAP records and link sedimentation on the New Jersey slope with orbitally controlled climate change. Although the relationship is best developed at Site 902, spectral analysis of the magnetic susceptibility records for Holes 903A and 904A support the interpretation of climatic forcing of sediment deposition at these sites. High coherency at the 100, 41, and 23-k.y. periodicities at Sites 902 and 903 indicate that our correlations are sound. The Site 904 correlations are less certain, though comparison to the SPECMAP stack suggests that our correlations are reasonable to at least the stage level. We suggest that the GRAPE signal for the Leg 150 sites reflects changes in grain size and variations in opal and carbonate content. Correlations of opal and carbonate content and the weight percentage of sand to the GRAPE records at Hole 902D indicate a consistent relationship between physical properties records and sedimentological components.

Our studies suggest that Pleistocene sedimentation on the New Jersey slope was dominated by regular, climatically driven changes in grain size. This affects sediment density and porosity and permits the construction of substage-level stratigraphies (e.g., Sites 902 and 903). Occasional mass-wasting events have blurred these changes in portions of the physical properties records (e.g., the upper 13 m of Site 904), but chronologies to the stage level can still be constructed. The consistent relationship between the physical properties records and glacial–interglacial cycles at all three sites illustrates the utility of GRAPE as a valuable stratigraphic tool, even in an environment as complex as the New Jersey slope.

INTRODUCTION

The primary objective of Ocean Drilling Program (ODP) Leg 150 was to date Oligocene to Miocene sequences on the New Jersey Margin. Although the Pleistocene of this region (Fig. 1) was known to provide an excellent section with clearly prograding clinofolds (plate 1 in Mountain, Miller, Blum, et al., 1994), we did not anticipate that a Pleistocene chronology would be readily obtained for these sediments due to a discontinuous record. However, shipboard analyses showed distinct cycles in sediment physical properties (GRAPE and magnetic susceptibility), which could be visually correlated with the SPECMAP middle to late Pleistocene oxygen isotope record (Imbrie et al., 1984) (Figs. 2–4), particularly in the upper part of Hole 902C (0–65 mbsf) (Fig. 2). Preliminary age models for the Pleistocene sections of Leg 150 Sites 902, 903, and 904 were constructed using calcareous nannofossil biostratigraphy (see Mountain, Miller,

Blum, et al., 1994) in order to relate the physical properties records to the SPECMAP time scale. These shipboard correlations suggest that high GRAPE and magnetic susceptibility values correlate with glacial periods and that low GRAPE and magnetic susceptibility values are associated with interglacial periods. This study presents an improved chronology for New Jersey slope Sites 902 (811 m water depth), 903 (444 m water depth), and 904 (1123 m water depth) using astronomically calibrated GRAPE and magnetic susceptibility records tied to calcareous nannofossil stratigraphy. We calibrate the glacial–interglacial changes in physical properties to sedimentological variations.

PREVIOUS STUDIES

GRAPE is an effective stratigraphic tool because it is a continuous, high-resolution (2 cm) measure of wet bulk density, which provides a rapid, nondestructive record of the lithologic variability of a core. It is particularly valuable for shipboard studies because GRAPE data can be used to identify missing section between successive cores by comparing records from the multiple holes drilled at each site (e.g., Hagelberg et al., 1992; Farrell et al., 1995). In pelagic environments, variations in GRAPE are caused by density and porosity changes resulting from fluctuations in the biogenic sediment content (opal and carbonate) (Herbert and Mayer, 1991; Mayer, 1991). This variation, coupled with the high resolution, is the foundation for using GRAPE as a stratigraphic tool. For example, the Leg 138 GRAPE

¹Mountain, G.S., Miller, K.G., Blum, P., Poag, C.W., and Twichell, D.C. (Eds.), 1996. *Proc. ODP, Sci. Results*, 150: College Station, TX (Ocean Drilling Program).

²Department of Geological Sciences, University of South Carolina, Columbia, SC 29208, U.S.A. Christensen: bac@paleo.geol.sc.edu

³Department of Geological Sciences, University of California, Santa Cruz, Santa Cruz, CA 95064, U.S.A.

⁴Department of Geological Sciences, Rutgers University, Piscataway, NJ 08855, U.S.A.

⁵Lamont-Doherty Earth Observatory, Columbia University, Palisades, NY 10964, U.S.A.

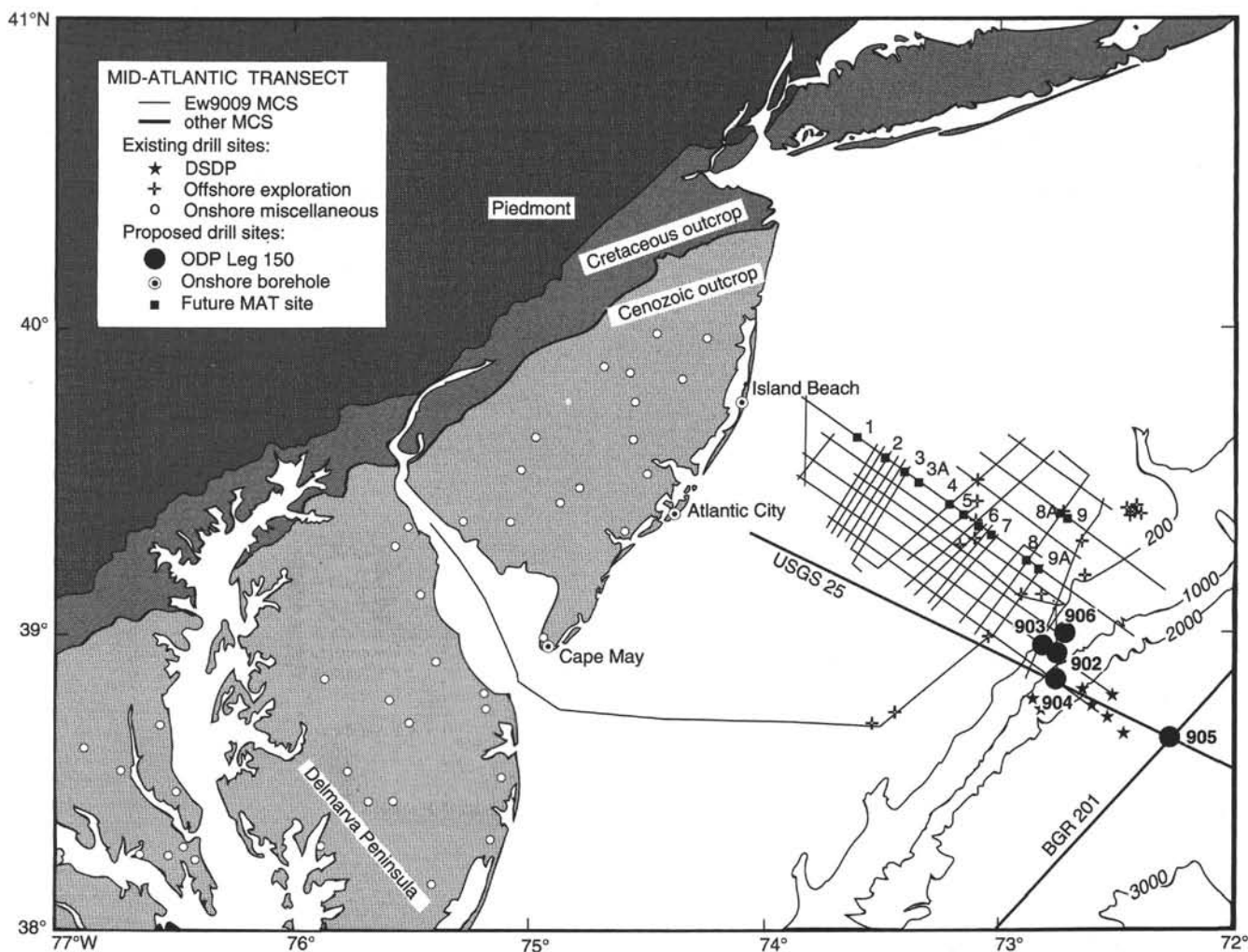


Figure 1. Location map of Leg 150 drill sites.

signal is a record of equatorial Pacific glacial–interglacial carbonate variations. This relationship between carbonate content and climate was used to develop astronomically calibrated high-resolution stratigraphies from the GRAPE records (Shackleton et al., 1992). However, in areas dominated by hemipelagic sedimentation, the primary component of the GRAPE signal (opal and carbonate variations) is diluted by terrigenous material. For instance, in the North Atlantic Ocean, GRAPE data reflect glacial dilution of the carbonate content by ice-rafted debris (IRD), so that highest GRAPE values indicate glacial intervals (Herbert and Mayer, 1992). Similarly, the Leg 150 GRAPE data provide a record of Pleistocene variations in the influx of terrigenous sediments to the New Jersey Margin.

Lowered sea level during glacial periods resulted in the deposition of large volumes of terrigenous material on the New Jersey slope (Cousin and Thein, 1987). The presence of mica, wood fragments, and transported shelf benthic foraminifers, in association with increased volumes of sand (Mountain, Miller, Blum, et al., 1994), implies that glacial sedimentation at the Leg 150 core sites was dominated by deposition of displaced sediments during lowered sea level. At the Leg 150 sites, there is a positive correlation between the physical properties values (GRAPE and magnetic susceptibility) and terrigenous sediment content. High GRAPE and magnetic susceptibility values are associated with increased sand content and are correlated to glacial periods (Fig. 5; see also Mountain, Miller, Blum, et al., 1994). Conversely, interglacial sedimentation is characterized by low physical properties values, reduced amounts of coarse-grained terrig-

enous material, and increased percentages of biogenic components (Fig. 5; see also Mountain, Miller, Blum, et al., 1994).

The link between GRAPE and climate change suggested in the sediment record is substantiated by correlations of the Leg 150 physical properties records to Stages 5–16 of the SPECMAP oxygen isotope record and is best expressed at Site 902 (Figs. 2, 6). The relationship between GRAPE and glacial–interglacial climate change inferred from the shipboard chronologies (Mountain, Miller, Blum, et al., 1994) allowed correlation of the physical properties records to the SPECMAP stack at the substage level over much of the middle Pleistocene section, particularly for Stages 5–8. The preliminary success of GRAPE as a correlation tool in a dynamic environment such as the New Jersey slope was surprising, considering the potential complexity of the system (e.g., downslope transport and debris-flow deposits could obscure the glacial–interglacial signal). The good visual correlation of the GRAPE and magnetic susceptibility records with the SPECMAP oxygen isotope curve suggests that changes in deposition of sand at these three sites are climatically driven and are more predictable than we had anticipated.

OBJECTIVES OF THIS STUDY

The purpose of this study was to generate astronomically tuned stratigraphies for Sites 902, 903, and 904 at the oxygen isotope substage level. Specifically, we hoped to improve the precision of our

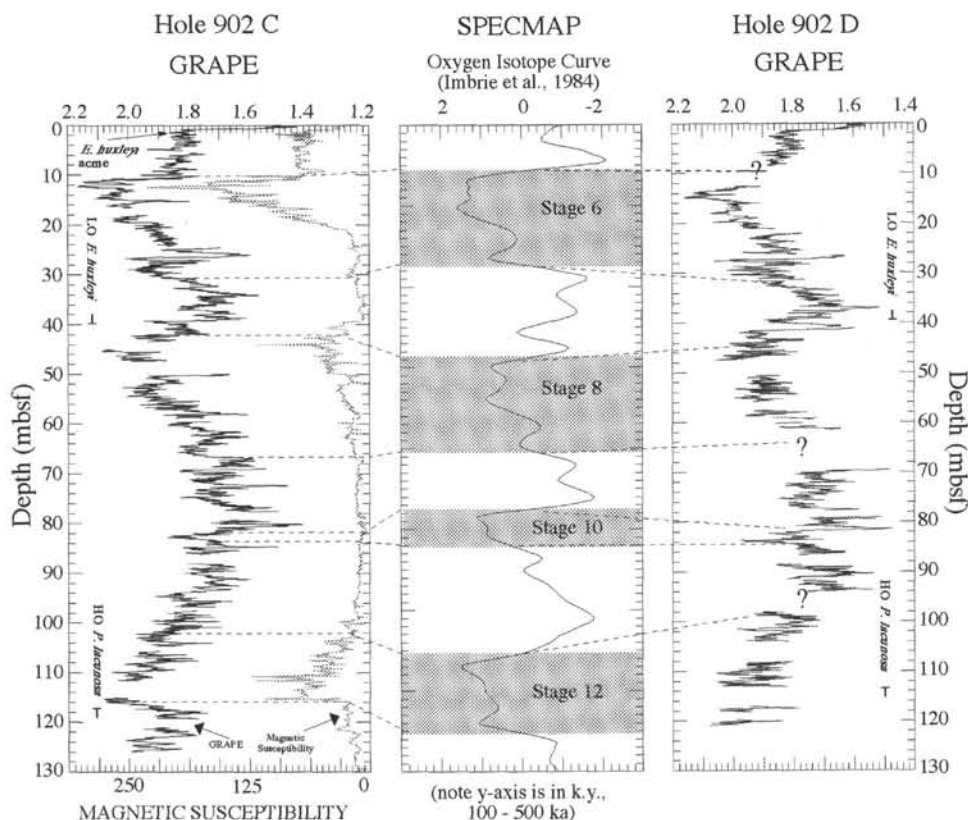


Figure 2. Site 902 GRAPE and magnetic susceptibility records vs. depth. GRAPE and magnetic susceptibility records for Hole 902C and GRAPE for Hole 902D are shown against the SPECMAP oxygen isotope time scale (Imbrie et al., 1984). (Note that the SPECMAP record is plotted against age, 100–500 ka.) Nannofossil datums constrain the ages to between Stages 5 and 12. There is a striking similarity between the GRAPE and magnetic susceptibility records and SPECMAP. Visual correlations between the high physical properties values and glacial stages, and between low physical properties values and interglacial stages, provided the foundation for the shipboard correlations.

initial shipboard correlations by tuning the physical properties records to the SPECMAP $\delta^{18}\text{O}$ stack (Imbrie et al., 1984) and by testing our age models by spectral and cross-spectral analysis of the physical properties and the SPECMAP records. Because the Site 902 record is the most complete and has the best visual correlation to the SPECMAP record, our primary goal was to establish the relationship between these two records at Hole 902C and then extend it to Sites 903 and 904. The visual correlation at Site 904 is blurred by a probable slump in the uppermost cores, and as a result, we did not expect to improve the correlation beyond the stage level. We also attempted to evaluate the relationship between GRAPE and the terrigenous and biogenic sediment components using records of opal and carbonate concentrations and the weight percentage of sand.

METHODS

Missing Section

Physical properties records were evaluated for the Pleistocene sections of Holes 902C (119 mbsf), 902D (121 mbsf), 903A (350 mbsf), 903B (148 mbsf), and 904A (110 mbsf) (Fig. 1). Normally, multiple holes are drilled at each site and composite sections are generated to determine whether section is missing from individual holes. Because the primary objectives of Leg 150 did not include the complete recovery of the Pleistocene section, only one additional hole was drilled through the Pleistocene interval (Site 902), a short second hole was recovered at Site 903, and no additional holes were drilled at Site 904. The lack of multiple holes at the Leg 150 sites forced us to evaluate our high-resolution records without the benefit of composite sections. However, we infer from correlation to the SPECMAP stack (Figs. 2, 3, 6; Table 1) that Stages 5–12 are present at Site 902,

with the exception of a condensed Stage 10 interval, and that only 2 substages (7.1 and 8.5) are missing from Site 903.

The completeness of the Pleistocene interval of Hole 902C relative to Hole 902D is shown by comparing the GRAPE records of the two holes. The two records are quite similar (Fig. 7A). Although additional intervals may be missing, especially below ~60 mbsf, which cannot be identified due to gaps in the physical properties record, the lowest datum levels are consistent between the cores (highest occurrence of *P. lacunosa* at 116.32 mbsf in Hole 902C and 113 mbsf in Hole 902D), which suggests that any missing intervals are thin. One interval of ~4 m is missing from the Hole 902C section between ~32 and 34 mbsf (events I and II; Fig. 7A), which is expanded between I and II relative to Hole 902C (Fig. 7A). Also, a thin interval (~1 m) is missing in Hole 902C at ~81 mbsf (event IV; Fig. 7A) as evidenced by a single peak present in the Hole 902C GRAPE record rather than the double peak in the Hole 902D record. Little missing or condensed section at Hole 902D (III, ~55 mbsf; Fig. 7A) is inferred from comparison to the Hole 902C record.

Comparison of the filtered magnetic susceptibility records at Holes 903A and 903B (0–147.9 mbsf) suggests that little section is missing from the upper 150 m in Hole 903A (Fig. 7B). A gap in the physical properties record for Hole 903A is present between 62.7 and 78 mbsf. This gap in the Hole 903A record was replaced by the record (59.7 and 75 mbsf) from Hole 903B. We spliced a section from Site 903B (59.7 to 75 mbsf) into the record from Hole 903A (62.7–78 mbsf) based on a correlation of second-order fluctuations (Fig. 3). This splice did not alter the results of the statistical analyses, so the original Hole 903A record is retained for this study.

For the purposes of this study (improving the chronology to the substage level and establishing that deposition at our sites was modulated at Milankovitch band frequencies), the records, although

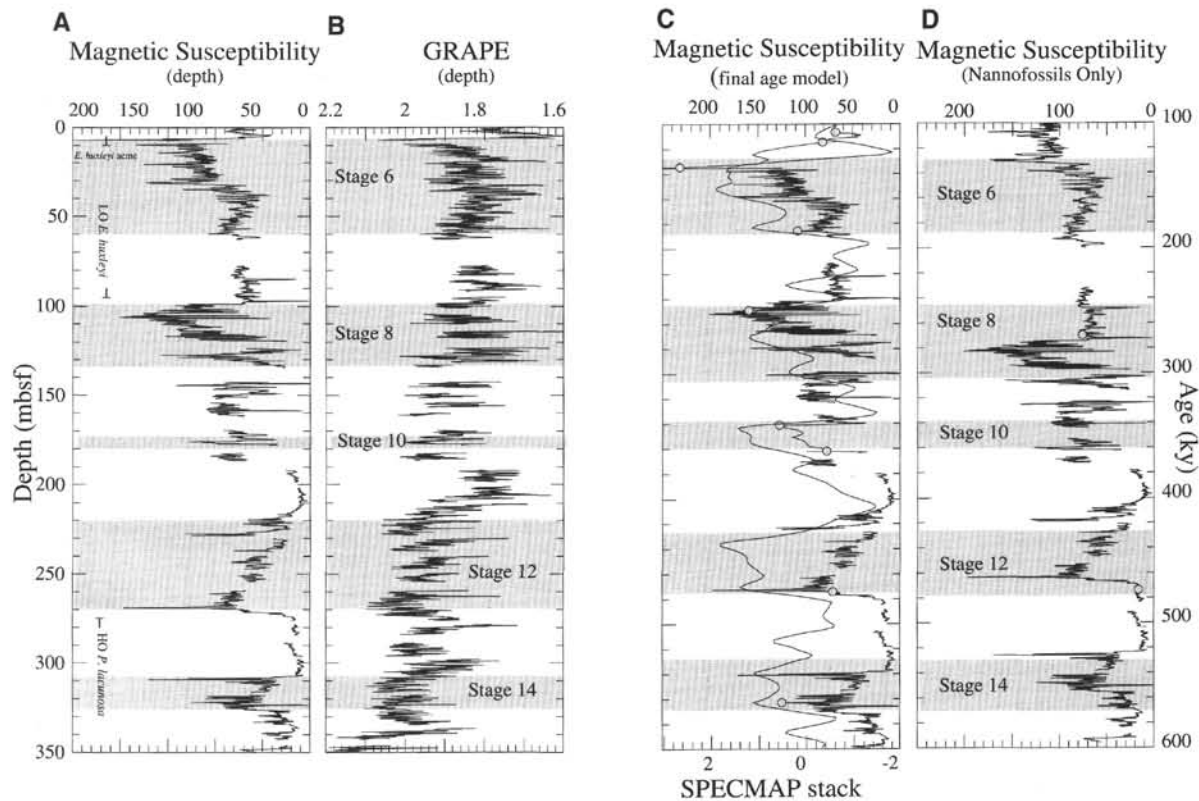


Figure 3. Site 903 physical properties vs. depth, and magnetic susceptibility age models. Glacial–interglacial variability is more apparent in the magnetic susceptibility record (A) than the GRAPE record (B). The amplitude of the change in the magnetic susceptibility record (A) allows for better visual correlation to the SPECMAP time scale (note that the SPECMAP record is plotted against age, 100–500 ka). Two age models are shown: the first is tuned to the SPECMAP record (C) and the second was calculated from nannofossil age datums only (D). Circles mark the control points used for correlation to the SPECMAP record. The difference between the two models is primarily the age of the *E. huxleyi* datum. Changing the age by ~30 k.y., from ~270 ka in (D), results in a shift in the position of the peak in magnetic susceptibility at ~105 mbsf, from the base of Stage 8 to the top of Stage 8. This change is in agreement with the correlation at Site 902 and is motivated by the uncertainty associated with the nannofossil datum due to dissolution and a large sampling interval.

punctuated with small gaps, are sufficient for our analyses. Statistical correlations are high (Table 1) for the 100-, 41-, and 23-k.y. periods, also suggesting that no significant amount of section is missing. In addition, because the sedimentation rates are so high at these sites (averages of 30 cm/k.y. at Site 902, 66 cm/k.y. at Site 903, and 25 cm/k.y. at Site 904), the small gaps in the records represent less time than a substage. For example, in Hole 902C, there is no evidence for any gaps in the record of more than ~4 m (30–34 mbsf). The sedimentation rate calculated for this interval is 34.78 cm/k.y. (Table 2), resulting in a maximum of 11 k.y. of missing time which is within the minimum sampling limit of the Nyquist frequency for the 23-k.y. periodicity ($N/2 = 12.5$). The only frequency that would be affected by this missing interval is the 19-k.y. period, and in fact, correlations at the 19-k.y. frequency are poor in Hole 902C in the interval older than Stage 8.

In addition to first- and second-order variations occurring at the stage and substage level, a third-order high-resolution variability also exists. We are confident from the association of the lithologic properties with the physical properties records, and their correlation to the SPECMAP stack, that the first- and second-order fluctuations (at the stage and substage levels) are related to climate change, but it is unclear if the third-order variations represent climatic events at sub-Milankovitch frequencies (e.g., Heinrich events; Bond et al., 1992), or if they represent simply random noise. If the third-order variability is unique to each core (e.g., small slumps) and not linked to climate, correlations between holes are rendered uncertain in the intervals punctuated by gaps. Additionally, the gaps represent less time than is relevant to our goal of correlating to the substage (≥ 19 k.y.) level. In-

stead of creating composite sections, the missing section was identified from comparison of the available records, assuming that there is no undetected coeval missing section in the holes.

AGE MODELS

The Pleistocene age models presented here were generated after refining the GRAPE and magnetic susceptibility data. First, GRAPE wet bulk density data were adjusted to fit correlative gravimetric and logging density records (see Hoppie, this volume) and then filtered (5-point moving average). The records were resampled at a 0.1-m interval for Holes 902C, 902D, 903A, and 904A. Physical properties records were compared to identify missing section. Magnetic susceptibility was used to establish a stratigraphy for Hole 903A (Fig. 3A) because the amplitude of the cyclicity in the magnetic susceptibility record is greater than that of the GRAPE record (Fig. 3B).

The physical properties records were first correlated visually to the SPECMAP oxygen isotope curve using the following nannofossil datum levels (Figs. 2–4): the highest occurrence (HO) of *P. lacunosa* (~474 ka, oxygen isotope Stage 12; Mountain, Miller, Blum, et al., 1994), the lowest occurrence (LO) of *Emiliania huxleyi* (~270 ka, oxygen isotope Stage 8; Gartner, 1977), and the *E. huxleyi* acme zone (~75–83 ka, oxygen isotope Stage 5; Gartner, 1990). The *E. huxleyi* acme zone was identified within the uppermost core at Sites 902 (0.2 mbsf) (Fig. 2) and 903 (<9.5 mbsf) (Fig. 3A), and may be present at Site 904 (≤ 8.5 mbsf) (Fig. 3A), indicating that a substantial unconformity exists and that most of Stages 2–5 were removed. These corre-

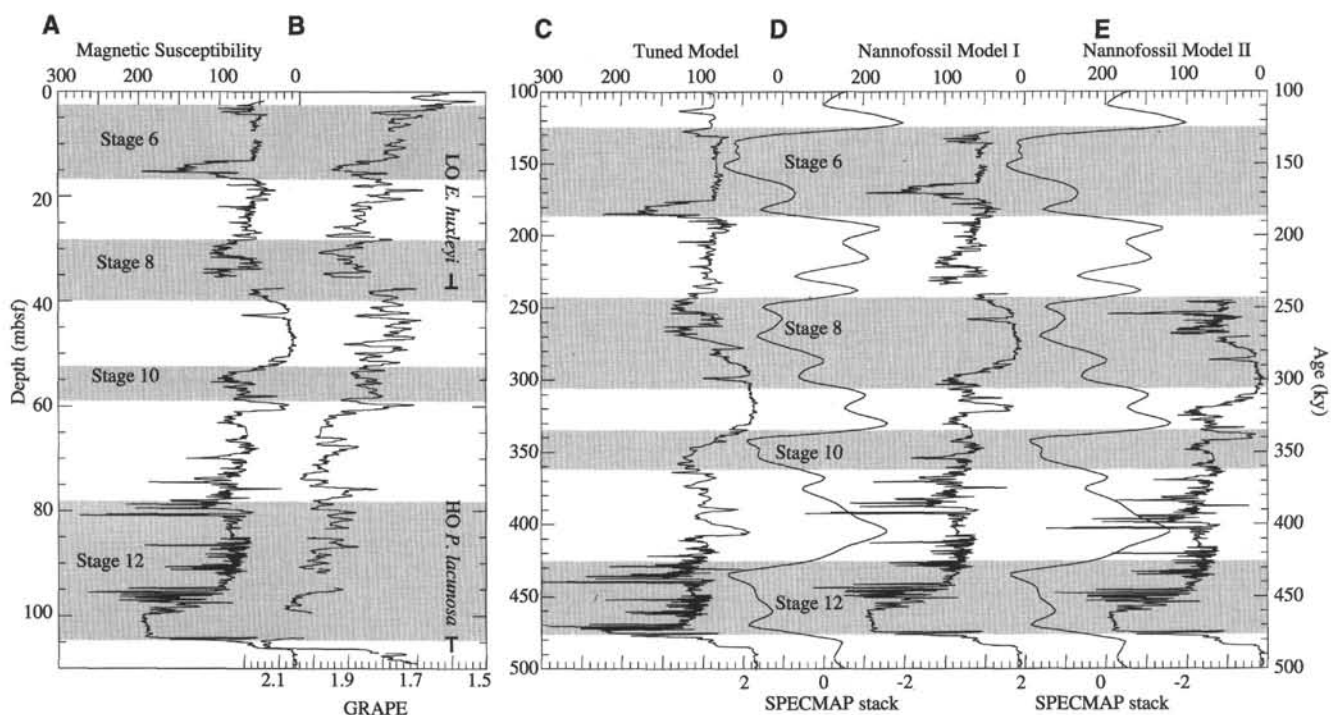


Figure 4. Site 904 physical properties vs. depth (left), and magnetic susceptibility age models (right). The visual correlation of the magnetic susceptibility (A) and GRAPE (B) data to the SPECMAP record is less apparent at Site 904 than in Hole 902C; however, tuning (C) improves correlations to at least the stage level. Two nannofossil-based age models are presented: Model I (D), for which we assume that the *E. huxleyi* abundance datum that is present in the uppermost core at Sites 902 and 903 is also present at Site 904, and Model II (E), for which we assume this datum is not present and that all of the record above ~50 mbsf is restricted to Stage 8.

lations established the initial stratigraphy to the oxygen isotope stage level. Major maxima and minima in the physical properties records (Table 2) were then used to calibrate the age model to the substage level, assuming constant sedimentation rates between control points (Table 2). The tuned physical properties records were compared to the age models generated using only the three nannofossil datums (Figs. 3, 4, 5) and adjusted to achieve the maximum visual correlation to the SPECMAP oxygen isotope curve. An alternative age model was generated for Hole 902C using additional control points to determine how increased tuning (to 1 control point every 9 m [average]; Table 2) affects the spectral analysis (Fig. 6; Table 1). Power spectra (Figs. 8, 9) were calculated for each age model ($\Delta t = 2$ k.y.). Cross-spectral results (Table 1) were calculated at 80% and 95% confidence intervals to determine the coherency of the variability at the precessional, tilt, and eccentricity periodicities.

Our correlations suggest that the LO of *E. huxleyi* is delayed at the Leg 150 sites by ~30 k.y. relative to the global datum (270 ka, Substage 8.4). Altering this age greatly improves correlations to the SPECMAP stack yet retains a lowest occurrence for *E. huxleyi* within Stage 8. We attribute the delay to a combination of dissolution, particularly in Stage 8 (S. Gartner, pers. comm., 1993), and dilution from the terrigenous component. An age-depth plot of the three nannofossil datums (Fig. 10) shows good agreement between Holes 902C and 902D, and between Sites 902 and 904, despite the potential problems associated with dissolution and dilution. An alternate explanation, that our correlations are off by one glacial stage, would place the LO of *E. huxleyi* in association with the Stage 9/10 boundary and require an unrealistic LO ~70 k.y. before the global first appearance. Because the Pleistocene nannofossil datums were identified from core-catcher samples at Sites 903 and 904, the large sampling interval (9.5 m) also lends some uncertainty to the datum levels. The similarity of the datum levels in Holes 902C, 902D, and 904A (Fig. 10) suggests, how-

ever, that the core-catcher datum estimates are reasonable, especially considering the high sedimentation rates at these sites. In addition, the LO of *E. huxleyi* is associated with a change from high to low physical properties values at the Stage 7/8 boundary at all three sites (Figs. 2, 3, 4). This similarity in the stratigraphic position of *E. huxleyi* provides further evidence that the LO is locally delayed, and that, despite dissolution and dilution, the datum levels are reasonable.

STRATIGRAPHY

Site 902

The similarity of the GRAPE and magnetic susceptibility records for Holes 902C and 902D to the SPECMAP oxygen isotope curve is apparent, even before tuning (Fig. 2). The good fit of the GRAPE record to the SPECMAP stack suggests that deposition was nearly continuous between isotope Substage 5.5 (5e) and Stage 12, with the exception of a condensed or missing Stage 10 (Figs. 2, 6). Nannofossil datums (LO of *E. huxleyi*, 39.33 mbsf in Hole 902C and 38.9 mbsf in Hole 902D, and the HO of *P. lacunosa*, 116.32 mbsf in Hole 902C and ~113 mbsf in Hole 902D) constrain the interval to between Stages 8 and 12, although Stage 10 is not well expressed at Site 902. A peak occurs in GRAPE values at 83 mbsf in Hole 902C (84 mbsf in Hole 902D). We interpret this peak as a condensed Stage 10. Three age models are presented for Hole 902C: one model was generated using only nannofossil datums (Fig. 6A) and the other two were created by tuning the physical properties records to the SPECMAP oxygen isotope curve (Fig. 6B, C). The tuned GRAPE records (initial and final; Fig. 6B, C) were developed from correlations based on the delayed LO of *E. huxleyi*, which greatly improved correlations to the oxygen isotope time scale (Table 1). The initial age model (Fig. 6B) used only 8 points to constrain Stages 5 (79 ka), 5.5 (122 ka), 6.5 (171

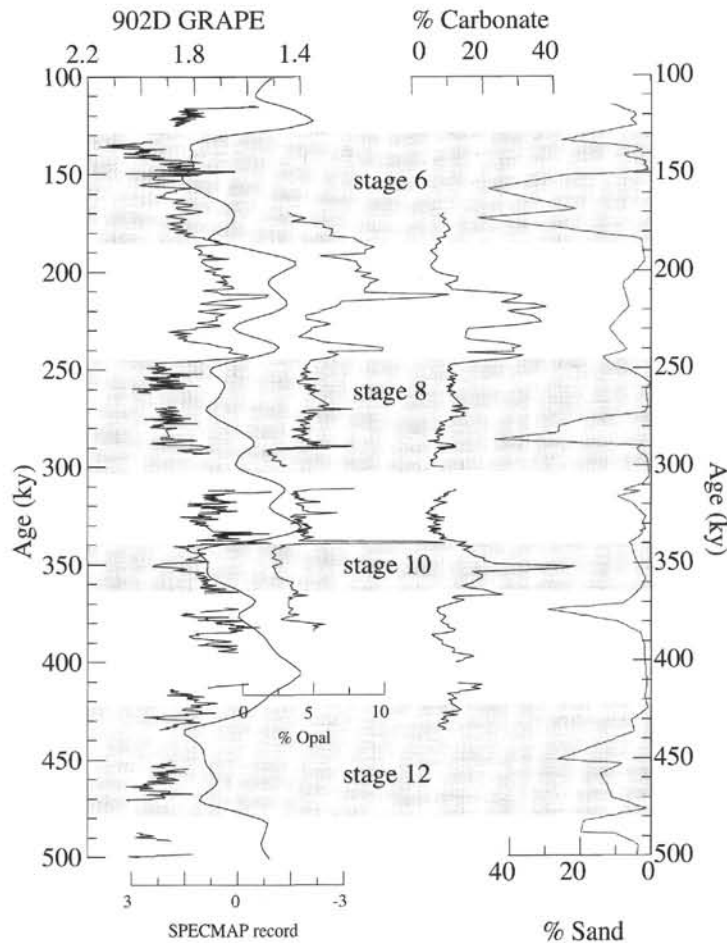


Figure 5. Hole 902D GRAPE and lithologic variables vs. age. High-resolution (0.2 m) opal and carbonate records and sand (0.4 m) are plotted against GRAPE data. Sand is calculated as weight percentage of sand, that is, the weight of the coarse fraction after washing through a 63- μ m sieve. There is a general correlation of high sand and GRAPE values with low carbonate and opal values (glacial), and lowest sand and GRAPE values with higher carbonate and opal (interglacial). These relationships suggest that the high GRAPE values in glacial intervals are the result of dilution of the biogenic components by the influx of the coarse fraction. Note that substage correlations of the SPECMAP record to the Hole 902D GRAPE record are limited by gaps in the physical properties record (Fig. 2).

ka), 8.0 (245 ka), 9.0 (303 ka), 10.0 (339 ka), 11.3 (405 ka), and 12.4 (474 ka), with a control point at approximately every 14.5 m. Substages agree roughly with the SPECMAP record, with the exception of Substages 6.6 and 8.6. Adding control points (Fig. 6C) to fix Substages 6.5, 7.1, 7.3, 7.4, and 9.4 improved correlations, yet tuning remains minimal (control points \sim 9 m).

Spectral analysis of the Hole 902C nannofossil-based chronology (Fig. 6A) reveals a small phase lag between the GRAPE and the SPECMAP records (Fig. 8C; Table 1). Cross-spectral analysis indicates that the lag is on the order of \sim 4 k.y. at the 19-k.y. band and \sim 10 k.y. at the 23-k.y. band (Table 1). Adjusting the age of the *E. huxleyi* datum and tuning the record to 8 substage points (Table 2) increases the coherency at the 100- and 41-k.y. periodicities but decreases it at the 19- and 23-k.y. periodicities (Table 1). This indicates that tuning to the stage boundary level results in a high degree of coherency of the first-order changes in the GRAPE record, but second-order (substage) correlations need refining. Tuning to the substage level (Fig. 6C; Table 2) increases coherency at the 100-, 41-, and 23-k.y. bands (Table 1). However, coherency at the 19-k.y. bandwidth is quite low (0.46) (Fig. 8A) and is associated with a high phase lag (\sim 9 k.y.) (Table 1). Restricting the spectral and cross-spectral analyses to the Stage 5 to 8 interval (84 and 300 ka) (Fig. 8B; Table 1) improves coherency and decreases the lag at the 19-k.y. periodicity to 1.6 k.y.

Some of this increase in coherency of the variance between 84 and 300 ka can be explained by the removal of the condensed Stage 10 from the analysis, but part of the increase may be related to a section missing below \sim 60 mbsf. The similarity of the nannofossil datum depths in Holes 902C and 902D and the comparison of the two records (Fig. 7) suggest that little of the section is missing down to Stage 8 (Fig. 2). This implies that gaps in the record below 65 mbsf, although small, affect the 1/19-k.y. frequency.

Unlike the highly coherent final age model for Hole 902C, the dominant peak in spectral density at Hole 902D occurs at a frequency of 1/31 k.y. (Fig. 9A). A similar cross-spectral analysis exists for the Hole 902C nannofossil-only age model (Fig. 8B) and indicates that substage tuning needs to be refined. Because the Hole 902D age model is affected by gaps in the GRAPE record (Figs. 2, 5), substage correlations are restricted in Stages 7 and 11. Again, we attribute the low 19-k.y. periodicity to aliasing due to gaps in the record, and the condensed Stage 10.

The relationship of GRAPE to the SPECMAP stack is strong, particularly through Stage 8 in Hole 902C. Only 13 control points were required for high coherency and spectral density of the tuned records (Fig. 8; Tables 1, 2). Based on the high coherency and low phase lag, in conjunction with a correlative low phase error, we infer that there is no substantial delay between the response of the sediments to cli-

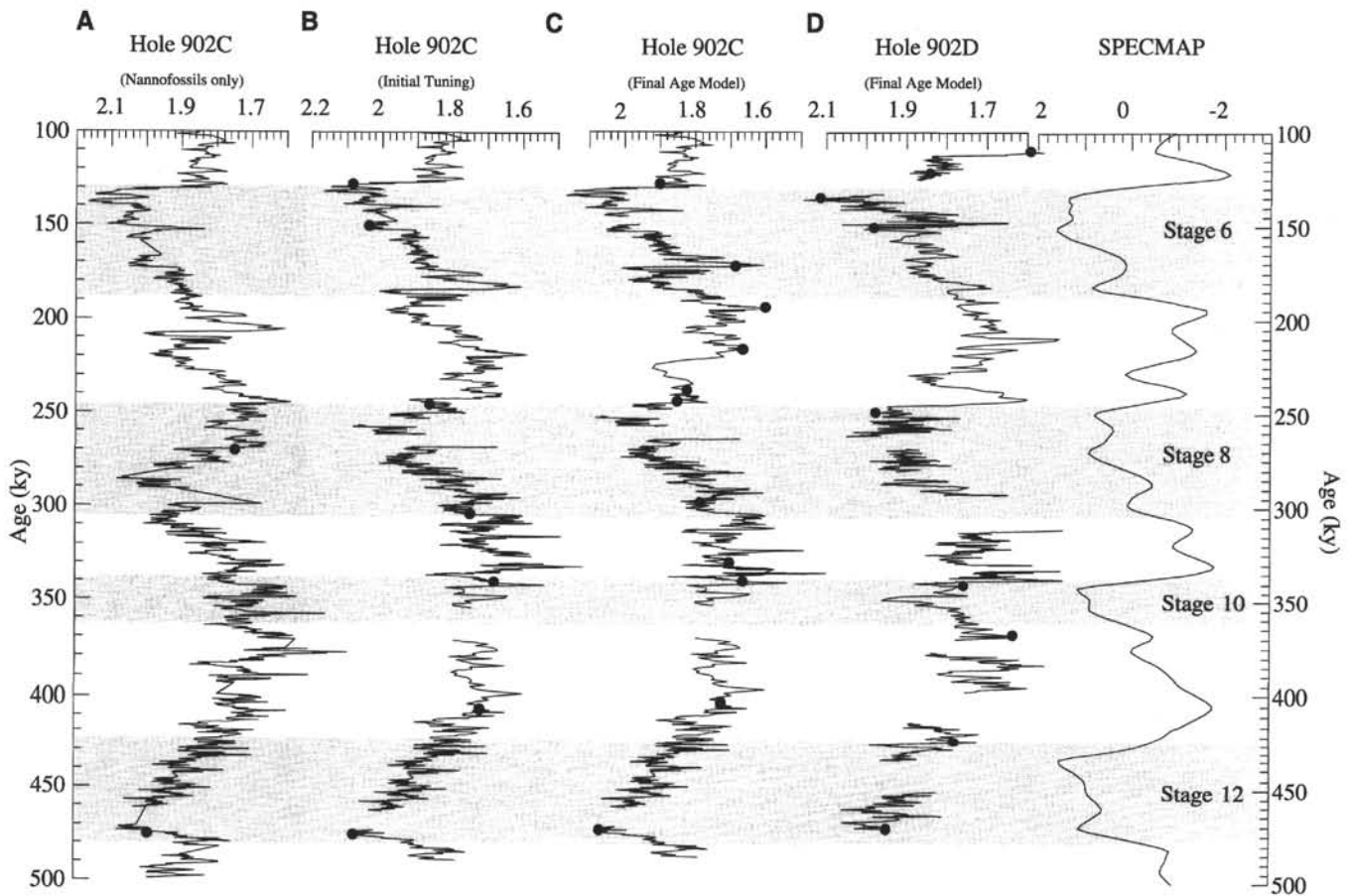


Figure 6. The tuned age models for Site 902. An initial age model (A) was generated using only the nannofossil datums in Hole 902C but resulted in low correlation to the SPECMAP record because of the stratigraphic position of *E. huxleyi* datum. We adjusted the age by ~30 k.y., and tuned the GRAPE data (B) to the SPECMAP record using 8 control points (Table 2). Circles mark the control points used for correlation to the SPECMAP record. The addition of 5 more control points (C) resulted in the highest correlation coefficients in the final age model (Table 1). An age model for Hole 902D (D) is also shown, but substage correlations are not as strong as at Hole 902C due to gaps in the GRAPE record.

mate change and the GRAPE record, and that the changes in the sediment content that drive the GRAPE signal is in phase with glacial-interglacial changes. Thus, large phase lags in the cross-spectral analyses indicate that tuning needs improvement. For example, correlations for Hole 902D are not as precise as those for Hole 902C because of the gaps in the record, resulting in a large phase lag (Table 1). Additional tuning should increase coherency and decrease the lag to a level similar to the lag in the Hole 902C final age model.

Site 903

The Pleistocene interval in Hole 903A is three times as thick as the Pleistocene section at Site 902. The magnetic susceptibility record (Fig. 3A) can be visually correlated to Stages 5.5 to 15 of the SPECMAP oxygen isotope record (Imbrie et al., 1984) (Fig. 3), despite gaps in the record. These gaps are due to gas expansion and reduced core recovery, particularly in the intervals 114–123.5, 133–142.5, 172.8–288.2, and 336.4–350 mbsf, complicating correlations of substages in those intervals.

Two age models were developed for Site 903: one based only on the three nannofossil datums (Fig. 3D), and a second on the tuned magnetic susceptibility record (Fig. 3C). The differences between the two age models are the stratigraphic positioning of the magnetic susceptibility peak at ~105 mbsf (Fig. 3A) and of Stage 10. The peak at 105 mbsf is correlated to the Substage 8.4/8.5 boundary using the nannofossil-based age model. Based on visual correlations to the

SPECMAP record (Fig. 3A) and comparison of the character of the Site 903 record to Hole 902C (Fig. 6), however, we correlate this peak to Substage 8.2 (Fig. 6C). We also correlate Stage 10 to a thin interval of high physical properties values at ~175 mbsf. The position of Stage 10 is equivocal but the ~175-mbsf maximum is present in both the GRAPE (Fig. 3B) and magnetic susceptibility (Fig. 3A) records in Hole 903A. Also, a condensed Stage 10 agrees with our interpretation of the Site 902 record.

The stratigraphic position of the LO of *E. huxleyi* (95 mbsf) is within an interval of low physical properties values interpreted as an interglacial. The interval could be correlated to Stage 9, but this would result in a local occurrence of *E. huxleyi* prior to the global first appearance in Stage 8. Alternatively, we can correlate this interval of low physical properties values to Stage 7, so that the LO of the taxon occurs after the global first occurrence. The large sampling interval (9.5-m core catchers) places this biostratigraphic datum within reasonable proximity of Stage 8.

Spectral densities of the tuned Hole 903A GRAPE and the SPECMAP records are similar (Fig. 9B), although lags between the two records are apparent and imply that the record requires further tuning. Nonetheless, a relatively strong correlation results from tuning 350 m of sediment with only 10 control points. Cross-spectral analysis of the nannofossil-based Hole 903A magnetic susceptibility time series and the SPECMAP record discloses a low coherency at the 100-k.y. periodicity and a large phase lag (11 k.y.) at the 23-k.y. period (Table 1). Coherency increases to moderate levels for the 23-, 41- and 100-

Table 1. Results of cross-spectral analysis between the GRAPE and magnetic susceptibility time series and the SPECMAP time scale.

Hole 902C GRAPE (final)				Hole 903A Magnetic susceptibility (final)			
Frequency	Coherency	Phase	Phase error	Frequency	Coherency	Phase	Phase error
1/100	.82	14.8	25.6	1/100	.80	20.2	27.1
1/41	.62	-11.0	41.1	1/41	.82	57.8	25.5
1/23	.94	-9.3	14.2	1/23	.70	-32.3	35.6
1/19	.46	172.3	52.8	1/19	.32	157.9	64.0
N/3 = 67, N = 202, BW = 0.0099 1/k.y.				N/3 = 82, N = 246, BW = 0.0061 1/k.y.			
Hole 902C GRAPE (final): 84–300 ka (Stages 5–8)				Hole 903A Magnetic susceptibility (spliced): N/3 = 258, N = 86, BW = 0.0077 1/k.y.			
Frequency	Coherency	Phase	Phase error	Frequency	Coherency	Phase	Phase error
1/100	.99	37.3	5	1/100	.81	20.9	26.6
1/41	.76	5.33	0.8	1/41	.83	56.6	24.7
1/23	.88	-11.5	20.1	1/23	.72	-36.3	33.4
1/19	.73	-30.9	32.7	1/19	.28	153.1	66.7
N/3 = 36, N = 109, BW = 0.018 1/k.y.				N/3 = 67, N = 202, BW = 0.0099 1/k.y.			
Hole 902C GRAPE (initial)				Hole 903A Magnetic susceptibility (nanofossil)			
Frequency	Coherency	Phase	Phase error	Frequency	Coherency	Phase	Phase Error
1/100	.79	-3.0	27.3	1/100	0.48	-5.6	51.5
1/41	.80	-39.2	69.3	1/41	0.78	141.2	28.5
1/23	.51	-2.8	49.6	1/23	0.44	-175.3	60.9
1/19	.35	49.6	61.6	1/19	0.83	39.2	24.8
N/3 = 70, N = 202, BW = 0.0099 1/k.y.				N/3 = 86, N = 258, BW = 0.0077 1/k.y.			
Hole 902C GRAPE (nanofossil)				Hole 904A Magnetic susceptibility (final)			
Frequency	Coherency	Phase	Phase error	Frequency	Coherency	Phase	Phase Error
1/100	.38	-33.5	59.2	1/100	.58	-29.8	44.2
1/41	.64	-9.8	39.6	1/41	.65	-18	38.8
1/23	.61	-154.4	42.0	1/23	.49	17.3	51.2
1/19	.96	-80.5	11.2	1/19	.77	68.2	30.1
N/3 = 70, N = 209, BW = 0.0095 1/k.y.				N/3 = 70, N = 210, BW = 0.0095 1/k.y.			
Hole 902D GRAPE (final)				Hole 904A Magnetic susceptibility (final): 170 to 270 ka			
Frequency	Coherency	Phase	Phase error	Frequency	Coherency	Phase	Phase Error
1/100	.75	8.4	31.2	1/1100	.93	-5.8	14.9
1/41	.81	70.6	69.1	1/41	.76	-10.3	30.4
1/23	.80	-16.4	27.5	1/23	.60	7.2	42.5
1/19	.54	-110.5	47.2	1/19	.61	24.2	41.8
N/3 = 65, N = 194, BW = 0.0077 1/k.y.				N/3 = 17, 51, BW = 0.039 1/k.y.			

Note: Cross spectra were performed at a 95% confidence interval, $\Delta t = 2$ k.y., N = number of data points, N/3 = number of lags. Bandwidth (BW) = $1.33/(N/3 \cdot \Delta)$.

k.y. periodicities with tuning (Fig. 9B; Table 1) and phase lags are low, with the exception of the 19-k.y. periodicity (8 k.y.). Splicing in section from Hole 903B had little effect on the analyses (Table 1).

Site 904

The record at Site 904 differs from those at Sites 902 and 903 in the lack of distinct glacial–interglacial variability in Stages 5–8. The interval between the top and ~40 mbsf can be interpreted as either a single glacial interval (all Stage 8), or two glacial intervals (Stages 6 and 8) with a thin interglacial Stage 7 between ~17 and 28 mbsf. Visual correlation suggests that Stages 6–8 are present, but that Stage 8 is not well developed. The Stage 5/6 boundary is characterized at Sites 902 and 903 by a strong peak in the physical properties measurements in core 1 (Figs. 3, 6) but the Stage 5/6 boundary at Hole 904A is not as pronounced (Fig. 4). The lower limit of this interval is constrained to Stage 8 by the LO of *E. huxleyi* (37.5 mbsf); however, the upper limit is not constrained by our data. The *E. huxleyi* acme may be present in Core 150-904A-1H (<8.5 mbsf), though only the core-catcher sample was analyzed. If the acme datum is present in the first core, as it is at Sites 902 and 903, then the youngest cored interval is constrained to between Stages 8 (or 6) and 5. If the acme is not present, then the youngest cored interval is constrained to Stages 8–6, or Stage 8.

Two nanofossil-based age models were generated to determine which interpretation of the physical properties record above 40 mbsf is most reasonable (Fig. 4). Assuming that the entire interval is Stage 8 (Fig. 3E) results in unusually high sedimentation rates, but a reasonable visual correlation to the SPECMAP stack. However, based on the records at Sites 902 and 903, we believe that an age model that includes Stage 6 (Fig. 3D) is more realistic. Sedimentation rates are similar to those at Site 902 in Stages 7 and 10 (Table 2) and a good visual substage correlation result from the using only the three age control points. Additional tuning (Table 2), to 10 control points, results in moderate coherencies (Table 2). Highest coherencies result from restricting the analysis to Substages 6.5–8.4 (170–270 ka).

SEDIMENTATION RATES

Average sedimentation rates at Sites 902 (30 cm/k.y.) and 903 (66 cm/k.y.) are very high. The high sedimentation rates allow us to correlate these two sites at the oxygen isotope substage level with a high degree of certainty, despite gaps in the physical properties records. The high coherency to the SPECMAP stack that results from using the age model derived from the revised age of the LO of *E. huxleyi* supports its use at Sites 903 and 904 (Fig. 11) and results in a reasonably similar slope at all three sites. A condensed Stage 10 is apparent

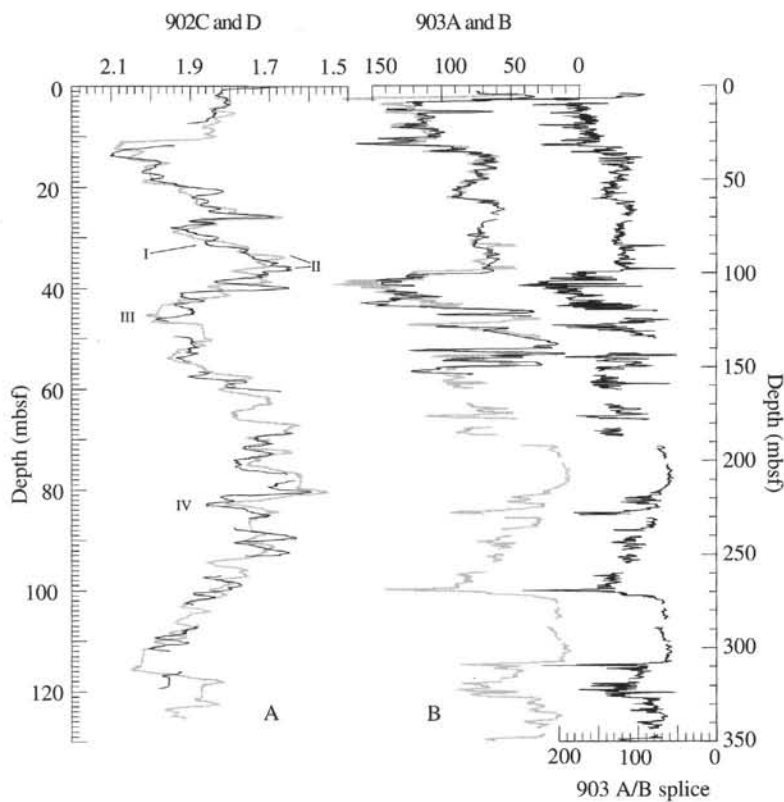


Figure 7. Missing section at Sites 902 and 903. Holes 902C (gray line) and 902D (black line) are plotted on the left. Holes 903A (gray line) and 903B (black line) are plotted on the right. The 903A/B spliced record is also shown for comparison.

at all three sites. Reduced sedimentation rates characterize Stage 7 in Holes 902C, 902D, and 904A, and although substage tuning was not performed in the Stage 7 interval of the Hole 903A record, sedimentation rates are lower than in Stage 6. The similarity of the three age models implies that the nannofossil biostratigraphy provides sufficient biostratigraphic control for the upper Pleistocene chronostratigraphy on the New Jersey slope.

LITHOLOGIC CONSTRAINTS ON GRAPE

Visual correlation of the Hole 902D GRAPE record with opal, carbonate, and sand records illustrates the relationship between glacial–interglacial changes and sediment composition on the New Jersey Margin. First-order changes in the biogenic sediment components are inversely proportional to the sand content and correlate to low GRAPE values (Fig. 4). During glacial periods, high volumes of sand transported to the slope diluted the biogenic opal and carbonate concentrations. Percentages of sand-sized material are highest during glacial Stages 6, 8, and 12, with the greatest percentages occurring during cold substages (e.g., 6.2, 6.4, 12.2) (Fig. 5). A spike in the sand record occurs within interglacial Stage 11 but is correlated to the cold Substage 11.2 (Fig. 5).

CONCLUSIONS

We improved our shipboard chronologies for Sites 902, 903, and 904 by visually tuning the physical properties record to the SPEC-MAP oxygen isotope record. We tested the tuning of the age models with spectral and cross-spectral analyses and show that first- and second-order variations in the physical properties records occur at orbital frequencies at Sites 902 and 903. Our chronology is less certain at Site 904 because the physical properties records of the uppermost sediments are apparently altered by a regional unconformity in Stage 5. However, spectral and cross-spectral analysis of the tuned age

model suggests our correlations are strong. We suggest that the variability in GRAPE at Sites 902, 903, and 904 is derived from relative changes in the concentrations of sand, opal, and carbonate, and are related to changes in sea level.

We had anticipated that slope sedimentation patterns would be irregular due to sporadic deposition and erosion. However, correlations to the oxygen isotope substage level suggests that the first- and second-order variations in the GRAPE are a function of climatically modulated deposition. The high correlation of the Leg 150 physical properties records to the SPEC-MAP oxygen isotope curve (Imbrie et al., 1984), especially at Sites 902 and 903, indicates that GRAPE is a valuable stratigraphic tool on the New Jersey Margin.

ACKNOWLEDGMENTS

The authors would like to gratefully acknowledge Terri Hagelberg for discussion and suggestions on processing GRAPE data and the Leg 150 Shipboard Scientific Party, especially our staff scientist, Peter Blum, and Stephan Gartner, who provided the calcareous nannofossil datums. Comments by reviewer C. Wylie Poag were invaluable, as were suggestions from N.J. Shackleton, W.L. Balsam, and D. Scott. A particularly in-depth review by D.M. Anderson greatly improved the manuscript. Special thanks also go to Kim Cockrell and Eric Tappa for laboratory assistance and to Jianning Le and Carol Pride for discussion and helpful reviews. This work was supported by a JOI/ USSAC Ocean Drilling Fellowship (Christensen).

REFERENCES

- Bond, G., Heinrich, H., Broecker, W., Labeyrie, L., McManus, J., Andrews, J., Huon, S., Janitschik, R., Clasen, S., Simet, C., Tedesco, K., Klas, M., Bonani, G., and Ivy, S., 1992. Evidence for massive discharge of icebergs into the North Atlantic ocean during the last glacial period. *Nature*, 360:245–249.

- Cousin, M., and Thein, J., 1987. Lithologic and geochemical changes across unconformities at Site 612, Deep Sea Drilling Project Leg 95, New Jersey Transect. In Poag, C.W., Watts, A.B., et al., *Init. Repts. DSDP*, 95: Washington (U.S. Govt. Printing Office), 549–564.
- Farrell, J.W., Murray, D.W., McKenna, V.S., and Ravelo, A.C., 1995. Upper ocean temperature and nutrient contrasts inferred from Pleistocene planktonic foraminifer $\delta^{18}\text{O}$ and $\delta^{13}\text{C}$ in the eastern equatorial Pacific. In Pisias, N.G., Mayer, L.A., Janecek, T.R., Palmer-Julson, A., and van Andel, T.H. (Eds.), *Proc. ODP, Sci. Results*, 138: College Station, TX (Ocean Drilling Program), 289–319.
- Gartner, S., 1977. Calcareous nannofossil biostratigraphy and revised zonation of the Pleistocene. *Mar. Micropaleontol.*, 2:1–25.
- , 1990. Neogene calcareous nannofossil biostratigraphy, Leg 116 (Central Indian Ocean). In Cochran, J.R., Stow, D.A.V., et al., *Proc. ODP, Sci. Results*, 116: College Station, TX (Ocean Drilling Program), 165–187.
- Hagelberg, T., Shackleton, N., Pisias, N., and Shipboard Scientific Party, 1992. Development of composite depth sections for Sites 844 through 854. In Mayer, L., Pisias, N., Janecek, T., et al., *Proc. ODP, Init. Repts.*, 138 (Pt. 1): College Station, TX (Ocean Drilling Program), 79–85.
- Herbert, T.D., and Mayer, L.A., 1991. Long climatic time series from sediment physical property measurements. *J. Sediment. Petrol.*, 61:1089–1108.
- Imbrie, J., Hays, J.D., Martinson, D.G., McIntyre, A., Mix, A.C., Morley, J.J., Pisias, N.G., Prell, W.L., and Shackleton, N.J., 1984. The orbital theory of Pleistocene climate: support from a revised chronology of the marine $\delta^{18}\text{O}$ record. In Berger, A., Imbrie, J., Hays, J., Kukla, G., and Saltzman, B. (Eds.), *Milankovitch and Climate* (Pt. 1), NATO ASI Ser. C, Math Phys. Sci., 126: Dordrecht (D. Reidel), 269–305.
- Mayer, L., 1991. Extraction of high-resolution carbonate data for paleoclimate reconstruction. *Nature*, 352:148–151.
- Mountain, G.S., Miller, K.G., Blum, P., et al., 1994. *Proc. ODP, Init. Repts.*, 150: College Station, TX (Ocean Drilling Program).
- Shackleton, N.J., and Shipboard Scientific Party, 1992. Sedimentation rates: toward a GRAPE density stratigraphy for Leg 138 carbonate sections. In Mayer, L., Pisias, N., Janecek, T., et al., *Proc. ODP, Init. Repts.*, 138 (Pt. 1): College Station, TX (Ocean Drilling Program), 87–91.

Date of initial receipt: 2 March 1995

Date of acceptance: 27 September 1995

Ms 150SR-01

Table 2. The control points and sedimentation rates used to generate age models by linear interpolation between GRAPE and magnetic susceptibility maxima and minima.

Event	Depth (mbsf)	Age (ka)	Sedimentation rate (cm/k.y.)
Hole 902C (nannofossil datums only):			
<i>Emiliana huxleyi</i> acme zone (top)	0.20	79	19.75
<i>E. huxleyi</i> acme zone (bottom)	0.99	83	20.50
LO <i>E. huxleyi</i>	39.33	270	37.74
HO <i>Pseudoemiliana lacunosa</i>	116.32	474	
Hole 902C (initial tuning):			
Top of acme zone	0.2	79	22.04
6.0	11.0	128	36.05
6.5	26.5	171	20.95
8.0	42.0	245	42.24
9.0	66.5	303	50.00
10.0	84.5	339	11.36
11.3	92.0	405	
HO <i>P. lacunosa</i>	116.0	474	
Hole 902C (final tuned age model):			
Top of acme zone	0.2	79	20.00
6.0	10.0	128	37.21
6.5	26.0	171	34.78
7.1	34.0	194	22.73
7.3	39.0	216	4.77
7.5	40.1	238	27.86
8.0	42.0	245	42.96
8.6	65.2	299	32.50
9.0	66.5	303	28.57
9.3	74.5	331	125.0
10.0	84.5	339	11.36
11.3	92.0	405	34.78
HO <i>P. lacunosa</i>		116	474.00
Hole 902D (tuned age model):			
5.4/5	0.3	110	88.57
5.5	6.5	122	57.08
6.2	13.9	135	94.31
6.4	29.0	151	13.27
8.2	42.0	249	43.90
9.3	78.0	331	50.00
10.2	83.0	341	14.29
11.0	86.0	362	24.59
12.0	101.0	423	25.00
12.4	113.0	471	
Hole 903A (tuned age model):			
5.4	4.0	107	28.75
5.5	6.3	122	3.00
6.2	6.9	135	103.92
7.0	59.9	186	70.00
8.2	104.0	249	78.26
10.2	176.0	341	5.24
11.0	177.1	362	58.43
HO <i>P. lacunosa</i>	270.0	474	82.95
14.4	322.0	563	49.12
16.0	350.0	620	
Hole 904A (tuned age model):			
Top acme zone	1.8	79	4.28
6.0	3.9	128	19.82
6.6	14.8	183	50.00
7.1	20.3	194	17.73
7.5	28.1	238	23.64
8.2	30.7	249	24.56
10.0	52.8	339	10.61
11.3	59.8	405	63.79
12.2	78.3	434	47.84
HO <i>P. lacunosa</i>	104.0	474	

Note: Ages for stage events are from Imbrie et al. (1984).

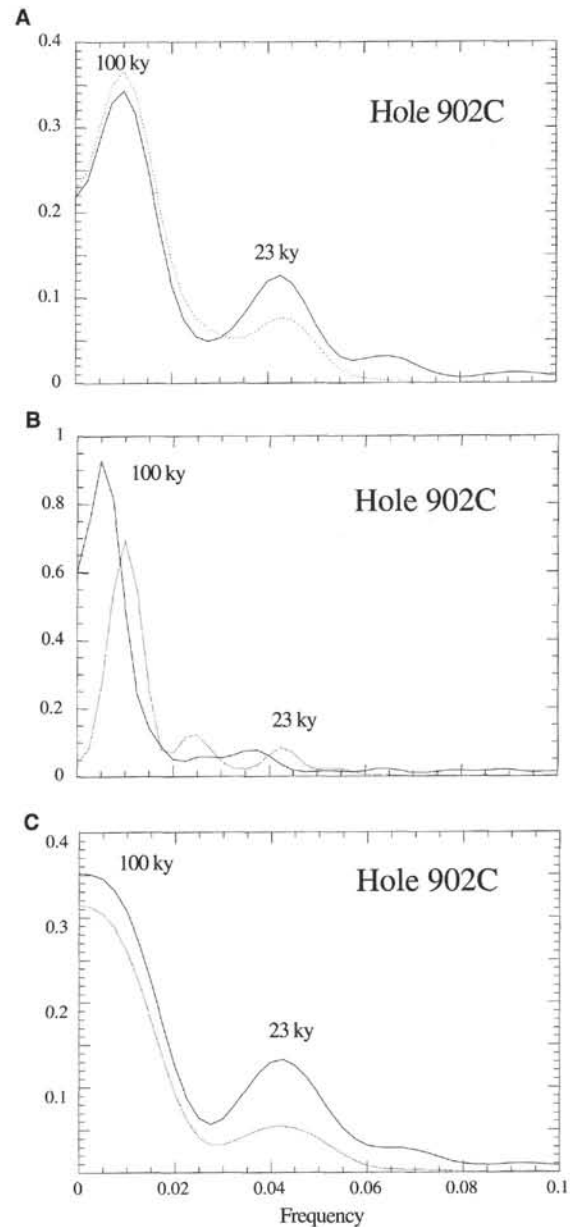


Figure 8. Power spectra for Site 902. Results of three analyses are shown: the final age model (A), the nannofossil-based age model (B), and Stages 5–8 of the final age model (C). For comparison, power spectra for the SPECMAP stack are also shown (dotted lines). Peaks are labeled if the variance was coherent at the 95% level in cross-spectral analyses.

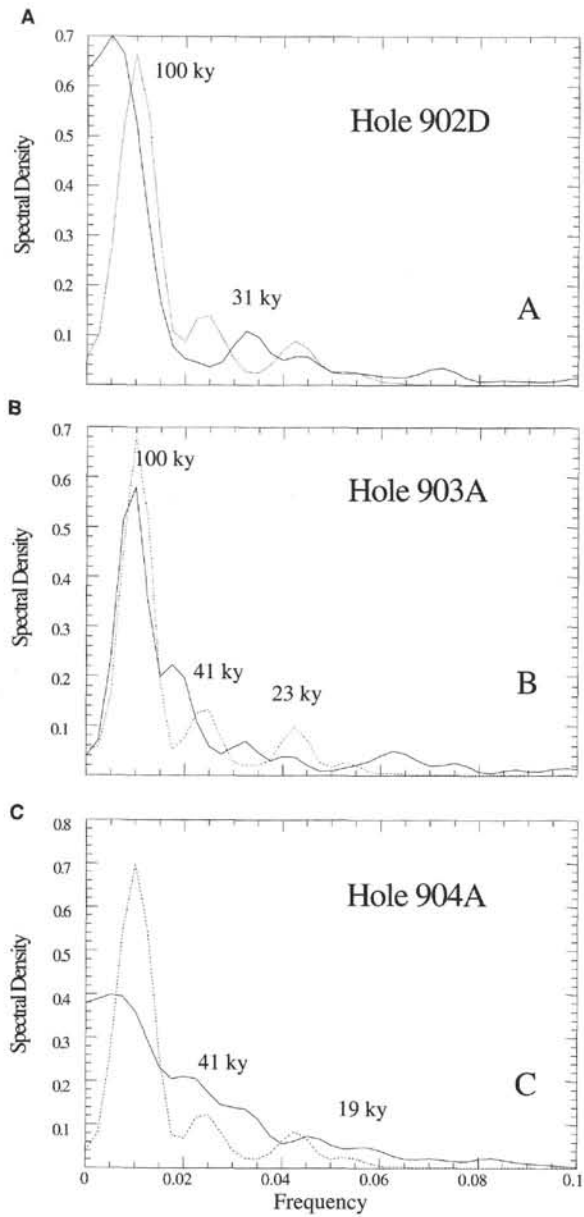


Figure 9. Power spectra for Holes 902D (A), 903A (B), and 904A (C). For comparison, power spectra for the SPECMAP stack are also shown (dotted lines). Peaks are labeled if there was coherency at the 95% level. Peaks are labeled if the variance was coherent at the 95% level in cross-spectral analyses for Holes 902D and at 80% for Holes 903A and 904A.

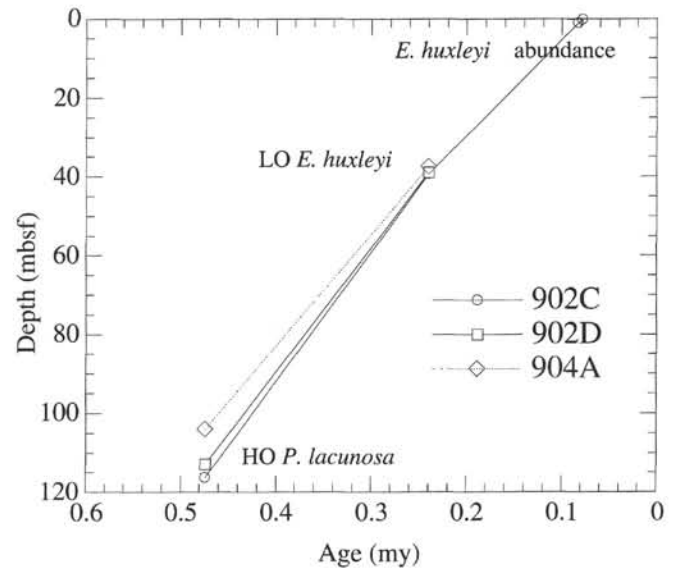


Figure 10. Age vs. depth plots for nannofossil datums (*E. huxleyi* abundance, LO *E. huxleyi*, and HO *P. lacunosa*) at Sites 902 and 904. The revised age of the LO of *E. huxleyi* is shown.

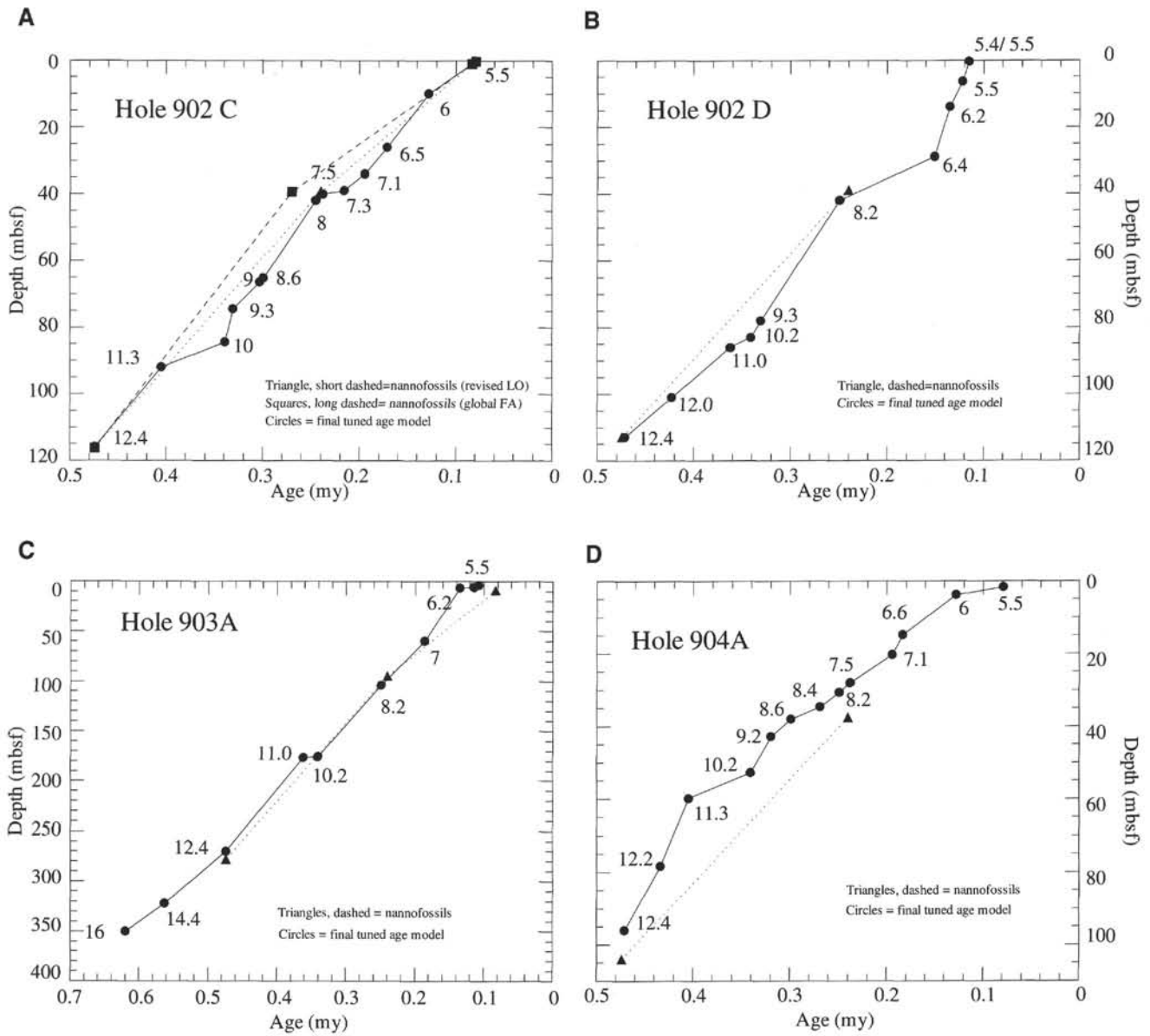


Figure 11. Age vs. depth plots for Sites 902, 903, and 904. An age model derived using the global first appearance datum (270 ka) is shown for Hole 902C (A). The final age models are compared to the nannofossil-based age model derived from the revised LO of *E. huxleyi* (240 ka) for Holes 902D (B), 903A (C), and 904A (D).